A HYDRATION MODEL OF AGGREGATE-MORTAR TRANSITION ZONE CONSIDERING PORE-PERMEATION COUPLING EFFECT BASED ON FRACTAL THEORY

by

Fan ZUO[a], Junqing LIU[b], and Chao LIU[a,b*]

[a] School of Civil Engineering, Xi'an University of Architecture and Technology, Xi'an, China
[b] School of Science, Xi'an University of Architecture and Technology, Xi'an, China

Original scientific paper
https://doi.org/10.2298/TSCI2203787Z

The high and non-uniform distributed porosity of the interfacial transition zone affects the macroscopic properties and failure behavior of concrete significantly, and it relies on the non-uniform water-cement ratio and pore-permeation coupling effect during hydration. However, current hydration models could not reveal the above facts. In this paper, water-cement distribution is derived, pore-permeation coupling effect is introduced based on fractal theory. Finally, a hydration model of the interfacial transition zone is established. A good agreement between the porosity prediction of interfacial transition zone and experimental data is found.

Key words: *fractal, interfacial transition zone, hydration, porosity*

Introduction

As the weak phase in concrete, the aggregate-mortar interfacial transition zone (ITZ) significantly affects the macroscopic properties and failure behavior of concrete [1-5]. Aggregate prevents the water permeation on the aggregate surface, which leads to the uneven distribution of the local water-cement ratio in ITZ. The non-uniformity of the water-cement ratio affects the water transportation, subsequently, the hydration procedure and microstructure of hydration product [2], which is called the side-wall effect [4, 6, 7]. The side-wall effect influences the hydration of ITZ, leading to high porosity and non-uniform distribution of porosity, which is considered as the reason for ITZ weakness [4, 6-8].

The ITZ has been studied experimentally through the nanoindentation technique, the mercury intrusion method and the electron microscopic observation method, and so on. Properties of hydrated ITZ, including porosity, microhardness, and elastic modulus, have been widely explored [1, 8, 9]. However, the influence of the hydration procedure on these properties has not been revealed directly.

In early theoretical research, the hydration mechanism and results were described qualitatively [4, 10]. In recent research, hydration of ITZ was approximately simulated by models of uniform cement-based material [2, 11-15]. Jiang *et al.* [13] promoted a numerical calculation model of porosity based on careful consideration of water-cement ratio, the thickness of cement and degree of hydration. Tan *et al.* [15] simulated hydration of transition zone between new and old mortars in recycled concrete, with the adoption of a traditional digital image-based

* Corresponding author, e-mail: chaoliu@xauat.edu.cn

model called CEMHYD3D model. Gao *et al.* [16] simulated the formation of ITZ micro-structure with two different hydration models, compared and discussed the two modeling results.

Due to the non-uniformity of the local water-cement ratio and water transportation in ITZ, hydration of ITZ differs from ordinary cement paste. Additionally, the pore feature in ITZ is changing in hydration procedure. Thus, ITZ could be regarded as a dynamic porous medium. In hydration of ITZ, water permeation affects pore features, and pore features affect permeability vice versa, but such pore-permeation coupling effect is not considered adequately in the open literature.

In this paper, a non-uniformly hydration model of the aggregate-mortar transition zone in concrete is established, porosity distribution of ITZ could be calculated. In this model, water transportation is introduced, local water-cement ratio and hydration rate are then modified. Fractal theory is adopted to characterize pore feature, the impact of pore-permeation coupling effect is then estimated. The validity of this proposed model is assessed by a comparison with experimental data of porosity distribution in ITZ.

Non-uniformly hydration model of ITZ

Modeling

As is shown in fig. 1, the interfacial transition zone is divided into n layers with the same thickness L. The thickness of the water layer on the aggregate surfaced is also set as L for simplification. It is assumed that the surface of aggregate is flat, and all layers are parallel. Water transports between layers. Along the direction perpendicular to the aggregate surface, n permeable cube cells with side length L are selected for calculation. The section area of each cell is $A = L^2$, volume $V = L^3$.

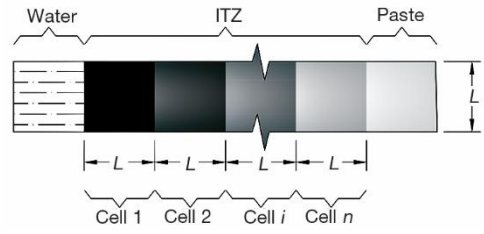

Figure 1. Permeable layers and cells in ITZ

Initial fraction of ITZ components

There are three kinds of components in ITZ or cement mortar paste: sand, cement, and water. Along the direction perpendicular to the aggregate surface, the fraction of cement and sand increases, water-cement ratio decreases. In cement mortar, the absolute volume fraction of a component is noted as, $\bar{\alpha}$, absolute mass fraction, m, relative mass fraction, m', initial water-cement ratio, ω_0. Subscript *sand* denotes sand, *ce* cement, *w* water. The mass ratio of cement and sand is:

$$\omega_{pa,0} = \frac{m'_{\mathrm{ce}}}{m'_{\mathrm{sand}}} = \frac{m_{\mathrm{ce}}}{m_{\mathrm{sand}}} = \frac{V_{\mathrm{ce}}\rho_{\mathrm{ce}}}{V_{\mathrm{sand}}\rho_{\mathrm{sand}}} \tag{1}$$

where V and ρ are volume and density, respectively.

The water-cement ratio in cement mortar paste is:

$$\omega_0 = \frac{m_{\mathrm{w}}}{m_{\mathrm{ce}}} = \frac{V_{\mathrm{w}}\rho_{\mathrm{w}}}{V_{\mathrm{ce}}\rho_{\mathrm{ce}}} \tag{2}$$

Combing eqs. (1) and (2), the absolute mass fraction of sand and cement in cement mortar is:

$$m_{\text{sand}} = \frac{m_{\text{sand}}}{m_{\text{sand}} + m_{\text{ce}} + m_{\text{w}}} = \frac{1}{1 + \omega_{pa,0} + \omega_0 \omega_{pa,0}} \tag{3a}$$

$$m_{\text{ce}} = \frac{m_{\text{ce}}}{m_{\text{sand}} + m_{\text{ce}} + m_{\text{w}}} = \frac{1}{\dfrac{1}{\omega_{pa,0}} + 1 + \omega_0} \tag{3b}$$

The absolute volume fraction of sand and cement is:

$$\bar{\alpha}_{\text{sand}} = \frac{\dfrac{m_{\text{sand}}}{\rho_{\text{sand}}}}{\dfrac{m_{\text{sand}}}{\rho_{\text{sand}}} + \dfrac{m_{\text{ce}}}{\rho_{\text{ce}}} + \dfrac{m_{\text{w}}}{\rho_{\text{w}}}} = \frac{1}{1 + \omega_{pa,0}\rho_{\text{sand}}\left(\dfrac{1}{\rho_{\text{ce}}} + \dfrac{\omega_0}{\rho_{\text{w}}}\right)} \tag{4}$$

$$\bar{\alpha}_{\text{ce}} = \frac{\dfrac{m_{\text{ce}}}{\rho_{\text{ce}}}}{\dfrac{m_{\text{sand}}}{\rho_{\text{sand}}} + \dfrac{m_{\text{ce}}}{\rho_{\text{ce}}} + \dfrac{m_{\text{w}}}{\rho_{\text{w}}}} = \frac{1}{1 + \rho_{\text{ce}}\left(\dfrac{\omega_0}{\rho_{\text{w}}} + \dfrac{1}{\omega_{pa,0}\rho_{\text{sand}}}\right)} \tag{5}$$

The absolute volume fraction of water is:

$$\bar{\alpha}_{\text{w}} = \bar{\alpha}_{\text{ce}} \omega_0 \frac{\rho_{\text{ce}}}{\rho_{\text{w}}} \tag{6}$$

At a point with distance d from the aggregate surface, the absolute volume fraction of cement could be calculated [17]:

$$\alpha_{\text{ce}}(d) = \bar{\alpha}_{\text{ce}}\left[1 + a_c\left(\frac{d-\delta}{\delta}\right)^2\right] 0 < d \le \delta \tag{7}$$

where $\bar{\alpha}_{\text{ce}}$ is determined by eq. (5), δ – the thickness of ITZ, a_c – a constant, a_c = –0.4959. The absolute volume fraction of sand could be calculated [18]:

$$\alpha_{\text{sand}}(d) = \bar{\alpha}_{\text{sand}}\left[1 - \exp\left(-\frac{d}{y_0}\right)\right] \tag{8}$$

where $\bar{\alpha}_{\text{sand}}$ is determined by eq. (4), y_0 is a constant, y_0 = 0.8.

The local water-cement ratio could be calculated:

$$\omega(d) = \frac{1 - \alpha_{\text{ce}}(d) - \alpha_{\text{sand}}(d)}{\alpha_{\text{ce}}(d)} \frac{\rho_{\text{w}}}{\rho_{\text{ce}}} \tag{9}$$

Fractal pore features

Key pore sizes

Relation among maximum pore diameter λ_{por}, minimum pore diameter λ_0, maximum water-filled pore diameter λ_{wat} and thickness of adsorption layer Γ [18] are shown in fig. 2.

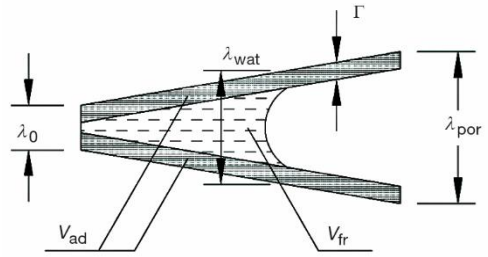

Figure 2. Key pore sizes in permeable cells; V_{ad} is the volume of adsorption water, and V_{fr} – the free water

In fig. 2, Γ is used as the thickness of 3 layers of water molecule [18], Γ = 0.0009 μm. The minimum and maximum permeable pore size λ_{min} and λ_{max} are calculated, respectively:

$$\lambda_{min} = \lambda_0 - 2\Gamma \tag{10a}$$

$$\lambda_{max} = \lambda_{por} - 2\Gamma \tag{10b}$$

According to reference [18], there are:

$$\lambda_0 = 0.002\ \mu m \tag{11}$$

$$\lambda_{por} = \lambda_0 \exp\frac{V_{por}}{a} \tag{12}$$

$$\lambda_{wat} = \lambda_0 \exp\frac{V_{fr}}{a} \tag{13}$$

where V_{por} is the pore volume in a permeable cell, V_{fr} – the volume of free water. The calculation of V_{por} and V_{fr} are shown in section *Water permeation based on pore features*.

According to fractal theory, the number of pores with a diameter larger than λ could be expressed [19]:

$$N(\geq \lambda) = \left(\frac{\lambda_{max}}{\lambda}\right)^{D_f} \tag{14}$$

where D_f is the fractal dimension. The number of pores with diameter in $[\lambda, \lambda + d\lambda]$ is:

$$-dN(\lambda) = D_f \lambda_{max}^{D_f} \lambda^{-(D_f+1)} d\lambda \tag{15}$$

Assuming the pore section is circular, the total section area of pores would be:

$$\bar{A} = -\int_{\lambda_{min}}^{\lambda_{max}} \frac{1}{4}\pi\lambda^2 dN(\lambda) = \frac{\pi D_f}{8-4D_f}\lambda_{max}^2\left[1-\left(\frac{\lambda_{min}}{\lambda_{max}}\right)^{2-D_f}\right] \tag{16}$$

For fractal porous media, porosity, ϕ, could be expressed as [19]:

$$\phi = \left(\frac{\lambda_{min}}{\lambda_{max}}\right)^{d_E - D_f} \tag{17}$$

where d_E is Euclidian dimension, d_E = 3 in the 3-D case. Then the pore size fractal dimension, D_f, is:

$$D_{\mathrm{f}} = 3 - \frac{\ln \phi}{\ln \lambda_{\min} - \ln \lambda_{\max}} \tag{18}$$

Porosity

Porosity in cement paste, ϕ, is defined:

$$\phi = \frac{V_{\mathrm{por}}}{V} \tag{19}$$

At time t_j, pore volume $V_{\mathrm{por},j}$ is composed of capillary water volume $V_{\mathrm{cap},j}$, and additional pore volume caused by chemical shrinkage, $\Delta V_{\mathrm{chsh},j}$ There is:

$$V_{\mathrm{por},j} = V_{\mathrm{cap},j} + \Delta V_{\mathrm{chsh},j} \tag{20}$$

where $\Delta V_{\mathrm{chsh},j}$ is calculated experimentally as 25% cement volume participating in hydration, [18]:

$$\Delta V_{\mathrm{chsh},j} = 0.25 \cdot 0.25 \Delta \alpha_j \frac{\rho_{\mathrm{ce}} \omega}{\rho_{\mathrm{w}} + \rho_{\mathrm{ce}} \omega} V \tag{21}$$

where $\Delta \alpha_j$ is the degree increment of hydration between time t_{j-1} and t_j.

If there are other components in cement mortar that could hydrate, the expansion of these hydration products reduces overall porosity. Denoting the mass fraction of these components as, m_o, density, ρ_o, volume fraction, $V_o = m_o/\rho_o$, the porosity of hydration product, ϕ_o. Considering the effect of aggregate and assuming that the degree of hydration expansion of these components is the same with cement, the whole porosity would be:

$$\phi_{\mathrm{act}}(V + V_o) = (1 - \alpha_{\mathrm{agg}})(\phi V + \phi_o V_o) \tag{22a}$$

$$V = V_{\mathrm{ce}} + V_{\mathrm{por}} \tag{22b}$$

where α_{agg} is volume fraction of aggregate. If $\phi_o = 0$, there would be:

$$\phi_{\mathrm{act}} = (1 - \alpha_{\mathrm{agg}}) \frac{V_{\mathrm{por}}}{V_{\mathrm{ce}} + V_{\mathrm{por}} + V_o} = (1 - \alpha_{\mathrm{agg}}) \frac{\phi}{1 + (1 - \phi) \dfrac{m_o}{m_{\mathrm{ce}}} \dfrac{\rho_{\mathrm{ce}}}{\rho_o}} \tag{23}$$

Water permeation based on pore features

Water volume in ITZ

At time t_j, the total water volume consists of three parts: the residual capillary water volume at the last time step, $V_{\mathrm{cap},j-1}$, the permeate water caused by the water pressure difference between adjacent cells, $V_{\mathrm{flow},j}$, and water consumed by hydration, $\Delta V_{\mathrm{hy},j}$. There is

$$V_{\mathrm{cap},j} = V_{\mathrm{cap},j-1} + V_{\mathrm{flow},j} - \Delta V_{\mathrm{hy},j} \tag{24}$$

Calculation of $V_{\mathrm{flow},j}$ is shown in section *Permeate water*. The $\Delta V_{\mathrm{hy},j}$ could be calculated:

$$\Delta V_{\mathrm{hy},j} = \Delta\alpha_j \omega_{\mathrm{cr}} \frac{\rho_{\mathrm{ce}}}{\rho_{\mathrm{w}} + \rho_{\mathrm{ce}}\omega} V \tag{25}$$

where $\omega_{\mathrm{cr}} = 0.4$ is the lowest water-cement ratio needed for complete hydration [18].

Capillary water volume, V_{cap}, is consisted of free water volume, V_{fr}, and adsorption water volume, V_{ad}, that is:

$$V_{\mathrm{cap}} = V_{\mathrm{fr}} + V_{\mathrm{ad}} \tag{26}$$

adsorption water volume, V_{ad}, does not participate in hydration, which could be calculated:

$$V_{\mathrm{ad},j} = 4a\left(-\frac{\Gamma}{\lambda} + \frac{\Gamma^2}{2\lambda^2}\right)_{\lambda_0}^{\lambda_{\mathrm{por}}} = 4a\Gamma\left(-\frac{1}{\lambda_{\mathrm{por}}} + \frac{1}{\lambda_0}\right) + 2a\Gamma^2\left(\frac{1}{\lambda_{\mathrm{por}}^2} - \frac{1}{\lambda_0^2}\right) \tag{27}$$

Here a is a constant, $a = 36 \cdot 10^9\ \mu\mathrm{m}^3$.

At time $t_{j=0}$, hydration does not begin yet, there is:

$$V_{\mathrm{por},j=0} = V_{\mathrm{cap},j=0} = \frac{\rho_{\mathrm{ce}}\omega}{\rho_{\mathrm{w}} + \rho_{\mathrm{ce}}\omega} V \tag{28}$$

Permeate water

The tortuosity of porous media with porosity ϕ is:

$$\tau(\phi) = 1 - 0.41\ln\phi \tag{29}$$

Denoting the capillary water head height as H', the tortuous length is:

$$H_t = \tau(\phi) H' \tag{30}$$

Then the capillary water volume would be:

$$V_{\mathrm{cap}} = H_t \bar{A} \tag{31}$$

Considering eqs. (30)-(31), water pressure in a permeable cell would be:

$$P = \rho_{\mathrm{w}} g H' = \rho_{\mathrm{w}} g \frac{V_{\mathrm{cap}}}{\tau(\phi)\bar{A}} \tag{32}$$

where $g = 9.8 \cdot 10^{-3} Ng^{-1}$. The water pressure difference between adjacent cells is denoted as ΔP. According to Hagen-Poiseuille' s Law, the flow of a single pore with diameter λ is:

$$q(\lambda) = \frac{\pi}{128} \frac{\Delta P}{\mu} \frac{\lambda^4}{L_t} \tag{33}$$

where μ is liquid viscosity, $\mu = 1.000 \times 10^{-15}\ \mathrm{Ns\mu m^{-2}}$ for liquid water, L_t is the tortuous length along permeation direction. There is:

$$L_t = L\tau(\phi) = (1 - 0.41\ln\phi)L \tag{34}$$

Integrating eq. (33) with respect to λ and substituting eq. (34) into integral result, the total flow in a single cell is obtained:

$$Q = -\int_{\lambda_{\min}}^{\lambda_{\max}} q(\lambda)\mathrm{d}N(\lambda) = \frac{\pi}{128}\frac{\Delta P}{\mu L}\frac{1}{1-0.41\ln\phi}\frac{D_\mathrm{f}}{4-D_\mathrm{f}}\lambda_{\max}^4\left[1-\left(\frac{\lambda_{\min}}{\lambda_{\max}}\right)^{4-D_\mathrm{f}}\right] \tag{35}$$

where D_f is the fractal dimension calculated by eq. (18).

At time increment $\Delta t_j = t_j - t_{j-1}$, the net flow of the k^{th} cell is:

$$V_{\mathrm{flow}:k,j} = (Q_{k-1} - Q_k)\Delta t_j \tag{36}$$

Influence of permeation on hydration depth

According to HYMOSTRUC hydration model, at time increment $\Delta t_j = t_j - t_{j-1}$, the increment of hydration depth is:

$$\Delta\delta_{in;x,j+1} = (\Delta\delta_{in;x,j+1})_0\Omega_1(x,\alpha_{x,j}) \tag{37a}$$

$$(\Delta\delta_{in;x,j+1})_0 = \frac{K_i F_1(\cdot)[F_2(\cdot)]^\lambda \Omega_2(\cdot)\Omega_3(\cdot)}{[(\delta_{x,j})^\lambda]^{\beta_1}} \tag{37b}$$

where K_j is a parameter related to the thickness of hydration product, F_1, F_2 – the parameters related to temperature, Ω_1 – a parameter related to particle embedding, Ω_2 and Ω_3 – parameters related to permeation.

Where Ω_2 is used for estimating the effect of pore state, defined as [18]:

$$\Omega_2 = \frac{\lambda_{\mathrm{wat}} - \lambda_0}{\lambda_{\mathrm{por}} - \lambda_0}\frac{\lambda_{\mathrm{por}}}{\lambda_{\mathrm{wat}}} \tag{38}$$

Meaning and calculation of $\lambda_{\mathrm{wat}}, \lambda_{\mathrm{por}}$, and λ_0 are shown in section *Key pore sizes*. The Ω_3 is used for estimating the effect of flow on the concentration of calcium ions. At time t_j, the water volume available for containing calcium ions, $v_{\mathrm{ca};j}$, is:

$$\text{water volume available} = \frac{\text{initial water mass} - \text{water mass consumed in hydration}}{\text{water density}} + \text{net flow}$$

that is:

$$v_{\mathrm{ca};j} = \frac{\omega m_{\mathrm{ce}} - \omega_{\mathrm{cr}}\alpha_j m_{\mathrm{ce}}}{\rho_{\mathrm{w}}} + v_{\mathrm{flow};j} \tag{39}$$

where α_j is current degree of hydration. At time t_j, the concentration of calcium ions is $(C_0)_j$, the volume of dissolved cement is $\Delta v_{\mathrm{ce};j}$, there is:

$$(C_0)_j = \frac{\Delta v_{\mathrm{ce};j}}{v_{\mathrm{ca};j}} \tag{40}$$

At time $t_j = 1$, concentration of calcium ion is:

$$(C_0)_{j=1} = \frac{\Delta v_{\mathrm{ce};j=1}}{\omega_0\dfrac{m_{\mathrm{ce}}}{\rho_{\mathrm{w}}}} \tag{41}$$

Assuming the concentration of calcium ions is stable, there is $(C_0)_j = (C_0)_{j=1}$. Combining eqs. (40) and (41), there is:

$$\Delta v_{\mathrm{ce};j} = \Omega_3 \Delta v_{\mathrm{ce};j=1} \tag{42}$$

Then

$$\Omega_3(\alpha_j) = \frac{\omega_0 - 0.4\alpha_j}{\omega_0} + \frac{v_{\mathrm{flow};j}}{\omega_0 \dfrac{m_{\mathrm{ce}}}{\rho_{\mathrm{w}}}} = \frac{\omega_0 - 0.4\alpha_j}{\omega_0} + \rho_{\mathrm{w}} \frac{v_{\mathrm{flow};j}}{\omega_0 m_{\mathrm{ce}}} \tag{43}$$

Verification and discussion

Three groups of tested porosity data in [16] were adopted for verification. The densities and mass fractions of components in binders are shown in tab. 1. The water-cement ratio of each binder was 0.3, 0.4, and 0.5, respectively, curing humidity was $95\% \pm 10\%$, curing temperature was 20 °C ± 1 °C, curing time was 56 days.

Table 1. Densities and mass fractions of components in binders [16]

	Cement	Slag	Filler
Specific density, [kgm^{-3}]	3120	2896	2650
Mass fraction in binder, [%]	60	20	20

Comparison between tested and calculated results are shown in fig. 3, and a good agreement is obtained. When ω_0 = 0.5, 0.4, the relative average error between tested and calculated results is 5.2% and 3.7%, respectively, the porosity calculation results show a slight overestimation compared to the experimental values. When ω_0 = 0.3, the relative average error is 13.3%, as in the former case, the porosity calculation results appear larger relative to the experimental values, but the degree of difference is greater compared to the former case.

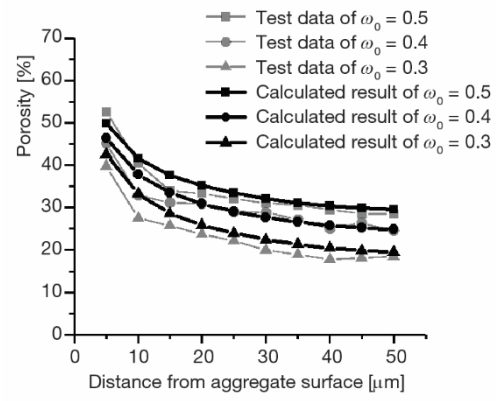

Figure 3. Comparison between tested and calculated results

The error may originate from the difference among initial water-cement ratio, ω_0. If ω_0 in cement mortar paste is relatively low, the humidity in pores would decrease obviously. Humidity correlates with adsorption water volume, V_{ad}, and adsorption thickness, Γ. Decreasing of humidity would lead to decreasing of V_{ad} and Γ, subsequently the decreasing of pore volume V_{por} and porosity ϕ.

Another possible effect of relatively low ω_0 is the overestimation of additional pore volume caused by chemical shrinkage, $\Delta V_{\mathrm{chsh},j}$. Water may distribute non-uniformly in ITZ. When ω_0 is relative lower, contact between cement and water may be inadequate, hydration may be insufficient. As is mentioned in section *Porosity*, $\Delta V_{\mathrm{chsh},j}$ is calculated experiencedly as 25% cement volume participating in hydration. Insufficient hydration may lead to lower $\Delta V_{\mathrm{chsh},j}$ than the theoretical prediction, subsequently the lower pore volume $V_{\mathrm{por},j}$ and actual

porosity ϕ_{act}. Therefore, the degree of porosity difference of $\omega_0 = 0.3$ is greater than that of $\omega_0 = 0.5, 0.4$.

Conclusion

In this paper, a hydration model of the interfacial transition zone is established. Based on fractal theory, pore features are described; water flow is derived roughly; the influence of permeation on hydration is estimated comprehensively by parameters Ω_2 and Ω_3. The model could reveal the fractal pore features and pore-permeation coupling effect during hydration and could be adopted to accurately calculate porosity distribution in ITZ. The predictions of porosity based on the proposed model are in good agreement with experimental data, the validity of the proposed model is verified.

The suggested model is suitable for ITZ when the water-cement ratio in cement mortar is 0.3-0.5. Further study could be extended to cases of a wider water-cement ratio.

Acknowledgement

The authors would like to acknowledge the financial support provided to this study by the National Natural Science Foundation of China (Grant No. 51878546), the Innovative Talent Promotion Plan of Shaanxi Province (Grant No. 2018KJXX-056), the Key Research and Development Projects of Shaanxi Province (Grant No. 2018ZDCXL-SF-03-03-02), the Science and Technology Innovation Base of Shaanxi Province (Grant No. 2017KTPT-19) and the Outstanding Youth Science Foundation Project of Shaanxi Province (2020JC-46).

References

[1] Andreas, *et al.*, Influence of Cement Type on ITZ Porosity and Chloride Resistance of Self-Compacting Concrete, *32* (2010), 2, pp. 116-120
[2] Bourdette, B., *et al.*, Transfer Properties of Interfacial Transition Zones and Mortars, *OPL, 370* (1994), p. 449
[3] Lee, K. M., *et al.*, A Numerical Model for Elastic Modulus of Concrete Considering Interfacial Transition Zone, *38* (2008), 3, pp. 396-402
[4] Scrivener, K. L., *et al.*, The Interfacial Transition Zone (ITZ) Between Cement Paste and Aggregate in Concrete, *12* (2004), 4, pp. 411-421
[5] Lutz, M. P., *et al.*, Inhomogeneous Interfacial Transition Zone Model for the Bulk Modulus of Mortar, *27* (1997), 7, pp. 1113-1122
[6] Breton, D., *et al.*, Contribution to the Formation Mechanism of the Transition Zone Between Rock-Cement Paste, *23* (1993), 2, pp. 335-346
[7] Bentz, D. P., *et al.*, Computer Simulation of Interfacial Zone Microstructure and Its Effect on the Properties of Cement-Based Composites, in: *Materials Science of Concrete IV*, Americ Ceramic Society, Westerville, O., USA, 1995, Chapter 5, pp. 155-200
[8] Nezerka, V., *et al.*, Micromechanical Characterization and Modeling of Cement Pastes Containing Waste Marble Powder, *195* (2018), Sept, pp. 1081-1090
[9] Mondal, P., Nanomechanical Properties of Cementitious Materials, Ph. D. thesis, Northwestern University, Evanston, Ill., USA, 2008
[10] Mehta, P. K., Monteiro, P., *Concrete: Microstructure, Properties, and Materials*, Mc Graw Hill, New York, USA, 2013
[11] Han, A. L., *et al.*, A Finite Element Approach to the Behavior of the ITZ, *764-765* (2015), May, pp. 3-7
[12] Jing, H., Stroeven, P. J. I. S., Properties of the Interfacial Transition Zone in Model Concrete, *12* (2004), 4, pp. 389-397
[13] Jiang, J. Y., *et al.*, Numerical Calculation on the Porosity Distribution and Diffusion Coefficient of Interfacial Transition Zone in Cement-Based Composite Materials, *Construction and Building Materials, 39*, (2013), Feb., pp. 134-138
[14] Yun, G., *et al.*, A Preliminary Numerical Study on ITZ in Cementitious Composites, in: *Multi-Scale Modeling and Char. of Infrastructure Materials*, Springer, New York, USA, (2013), pp. 99-108

[15] Tan, L., *et al.*, Hydration Process Modeling of ITZ Between New and Old Cement Paste, *109* (2016), Apr., pp. 120-127
[16] Gao, Y., *et al.*, The ITZ Microstructure, Thickness, and Porosity in Blended Cementitious Composite: Effects of Curing Age, Water to Binder Ratio and Aggregate Content, *60* (2014), Apr., pp. 1-13
[17] Nadeau, J. J. C., Water-Cement Ratio Gradients in Mortars and Corresponding Effective Elastic Properties, *32* (2002), 3, pp. 481-490
[18] Van Breugel, K., Simulation of Hydration and Formation of Structure in Hardening Cement-Based Materials, *2* (1991), 7, pp. 516-519
[19] Yu, B., *et al.*, A Fractal Permeability Model for Bi-Dispersed Porous Media, *45* (2002), 14, pp. 2983-2993

Paper submitted: January 6, 2021
Paper revised: August 17, 2021
Paper accepted: August 17, 2021